Available online at www.sciencedirect.com
ScienceDirect
Journal of Photochemistry and Photobiology A: Chemistry 197 (2008) 220–225
Journal of Photochemistry and Photobiology A:Chemistry
www.elsevier.com/locate/jphotochem

Photoinduced electron transfer dynamics in porphyrin donor dyads

James A. Hutchison [a], Toby D.M. Bell [a], Tapan Ganguly [a,1], Kenneth P. Ghiggino [a,*], Steven J. Langford [b,2], Nigel R. Lokan [b], Michael N. Paddon-Row [b,**]

[a] *School of Chemistry, University of Melbourne, Victoria 3010, Australia*
[b] *School of Chemistry, University of New South Wales, NSW 2052, Australia*

Received 14 November 2007; received in revised form 20 December 2007; accepted 26 December 2007
Available online 5 January 2008

Abstract

Intramolecular photoinduced electron transfer (PET) processes occurring in dyads with a free base porphyrin-tetraazaanthracene donor (P) and either a tetracyanonaphthoquinidodimethane (TCQ) or benzoquinone (BQ) acceptor linked by a rigid six σ-bond polynorbornane bridge ([6]) have been investigated. For **P[6]BQ**, PET in the polar solvent benzonitrile ($\varepsilon_s = 25.9$) occurs with a rate constant (k_{PET}) of 1.6×10^8 s^{-1} but is not evident in solvents less polar than tetrahydrofuran ($\varepsilon_s = 7.52$). For **P[6]TCQ**, highly efficient forward PET occurs in both polar and non-polar solvents ($k_{PET} > 2 \times 10^{10}$ s^{-1}). For **P[6]TCQ** the lifetime of the resulting charge-separated state decreases markedly with increasing solvent polarity. The results are discussed in the context of the likely mechanisms for electronic coupling and current theories for PET processes in such linked molecular systems.

Keywords: Photoinduced electron transfer; Charge-separated state lifetime; Porphyrin; Benzoquinone

1. Introduction

Photoinduced electron transfer (PET) reactions are ubiquitous in nature and are primary processes occurring in many photoexcited synthetic molecular and supramolecular systems. The roles of the donor and acceptor structure, intermolecular separation, relative orientation and surrounding environment on electron transfer dynamics remain topics of intense experimental and theoretical investigation [1–5]. Control of PET reactions is an essential requirement for the efficient operation of many molecular devices and light energy conversion and storage systems [6].

Of particular importance is acquiring an understanding of the factors that can affect the electronic coupling and driving force for electron transfer within a photoexcited donor–acceptor pair. In previous work we have demonstrated for a range of linked electron donor–acceptor molecular systems with interchromophore separations exceeding orbital overlap, the importance of through-bond interactions and the role of bridge structure on electronic coupling mechanisms [7–11]. In the present work we investigate PET dynamics in a covalently linked dyad bearing a free base porphyrin-tetraazaanthracene (P) donor and either a benzoquinone (BQ) or tetracyanonaphthoquinidodimethane (TCQ) acceptor. Connecting the two chromophores by a rigid polynorbornane bridge of six σ-bonds in length (molecules **P[6]BQ** and **P[6]TCQ**, Scheme 1) allow the donor–acceptor separation and orientation to be completely fixed. The geometry of the two systems is illustrated by the AM1 optimized geometry of **P[6]TCQ**, shown in Fig. 1. The different acceptors provide molecular systems with a large difference in PET driving force allowing the role of solvent on the PET dynamics to be investigated.

2. Experimental

Tetrakis(3′,5′-di-*tert*-butylphenyl)porphyrintetraazaanthracene[6]benzoquinone (**P[6]BQ**) was prepared as described previously [12]. Tetrakis(3′,5′-di-*tert*-butylphenyl)porphyrint-

* Corresponding author. Fax: +61 3 93475180.
** Corresponding author. Fax: +61 2 93856141.
E-mail addresses: ghiggino@unimelb.edu.au (K.P. Ghiggino), m.paddonrow@unsw.edu.au (M.N. Paddon-Row).
[1] Present address: Department of Spectroscopy, Indian Association for the Cultivation of Science, Calcutta 700032, India.
[2] Present address: School of Chemistry, Monash University, Clayton 3800, Australia.

1010-6030/$ – see front matter © 2008 Elsevier B.V. All rights reserved.
doi:10.1016/j.jphotochem.2007.12.026

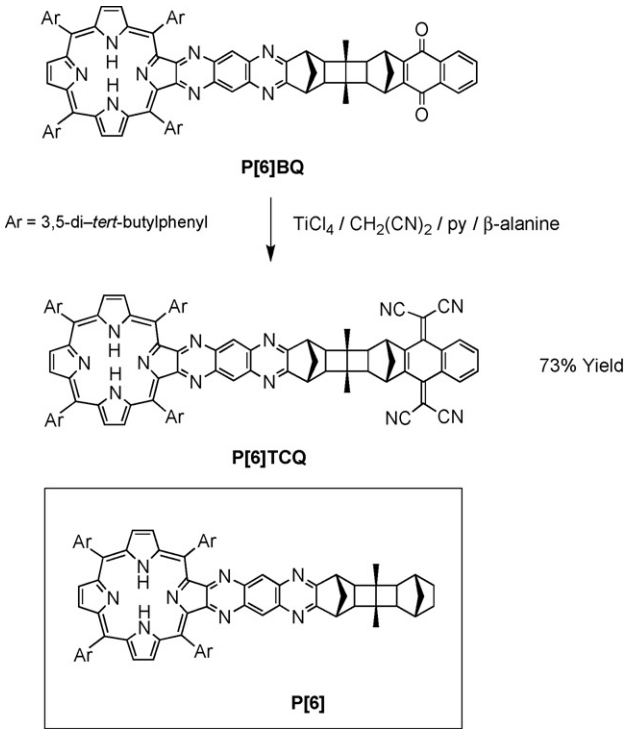

Scheme 1.

etraazaanthracene[6]tetracyanonaphthoquinidodimethane (**P[6]TCQ**) was prepared from **P[6]BQ** in 73% yield using a previously reported method for the conversion of norbornane and bicyclo[2.2.2]octane fused naphthoquinones to 5,12-bis(dicyanomethylidene)naphthalene systems (Scheme 1) [12]. m.p. > 300 °C. ^{1}H NMR ($CDCl_3$, 300 MHz): δ −2.40 (2H, s, inner NH); 1.17 (6H, s, CH_3), 1.52 (36H, s, *t*-Bu), 1.53 (36H, s, *t*-Bu), 1.46–1.70 (1H, underlying), 1.94 (1H, d, J = 10 Hz, CH), 2.19 & 2.30 (2H, ABq, J = 10 Hz, CH_2), 2.44 (2H, s, CH), 2.53 (2H, s, CH), 3.72 (2H, s, CH), 4.20 (2H, s, CH), 7.70 (m, 2H, BTCNQ-ArH), 7.80 (2H, t, J = 1.7 Hz, *meso*-ArH), 7.97 (4H, d, J = 1.7 Hz, *meso*-ArH), 8.02 (2H, t, J = 1.7 Hz, *meso*-ArH), 8.09 (4H, d, J = 1.7 Hz, *meso*-ArH), 8.44 (m, 2H, BTCNQ-ArH), 8.55 (2H, s, TAA-ArH), 8.77 (2H, s, β-pyrrolic H), 8.98 & 9.03 (4H, ABq, J = 4.7 Hz, β-pyrrolic H). ^{13}C NMR ($CDCl_3$, 300 MHz): δ 8.4, 30.7, 30.9, 31.0, 34.1, 38.9, 43.4, 43.5, 44.9, 47.0, 47.2, 78.7, 112.9, 113.1, 116.9, 119.8, 120.1, 122.0, 127.0, 127.4, 128.0, 131.5, 133.2, 137.1, 138.4, 138.7, 139.2, 139.7, 140.1, 144.6, 147.8, 148.1, 149.7, 152.1, 152.8, 154.0, 162.4, 164.1. ESIMS (50 V, +ive): m/z 1654.8 $[M+H]^+$, 827.6 $[M+2H]^{2+}$.

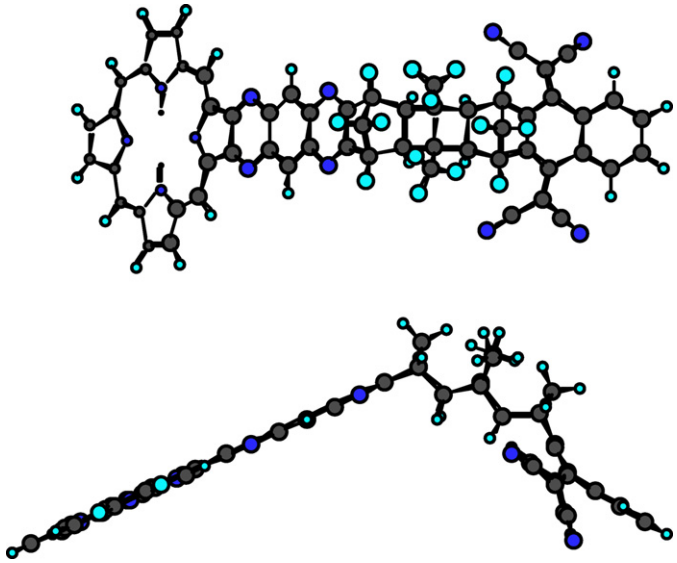

Fig. 1. AM1 optimized geometry of **P[6]TCQ**.

Solvents used for photophysical measurements were spectroscopic grade. Solutions in the appropriate solvent were degassed by multiple freeze-pump-thaw cycles before measurement. Absorption and fluorescence spectra were recorded on a Cary 50 spectrophotometer and Varian Cary Eclipse spectrofluorimeter, respectively. Fluorescence decay times were measured by the time-correlated single photon counting technique using a cavity-dumped, mode-locked Spectra Physics dye laser (3500) operating at 570 nm as the excitation source and detection and data analysis procedures as described elsewhere [9,10]. For transient absorption measurements, samples were excited by a Nd:YAG (Continuum NY-61) and OPO (Cassix BBO-3B) combination and transient absorption determined using a Rofin 150 W xenon lamp monitoring light source combined with a spectrograph (Acton Research Corporation SpectraPro-300i) and either a Princeton Instruments ICCD-MAX camera for recording transient spectra or photomultiplier tube/digital oscilloscope (Hamamatsu R928/Tektronix TDS-520) for decay measurements [9,10].

3. Results

An estimate of the driving force for photoinduced charge separation (ΔG_{CS}) in **P[6]BQ** and **P[6]TCQ** in various solvents can be determined from the Weller equation [13],

$$\Delta G_{CS} = e(E^{ox}(D) - E^{red}(A)) - E_{00} - X \quad (1)$$

where the term X accounts for the finite donor–acceptor separation (R_c), ionic radii (r^+, r^-) and solvent dielectric constant (ε_s),

$$X = \frac{e^2}{4\pi\varepsilon_0\varepsilon_s R_c} + \frac{e^2}{8\pi\varepsilon_0}\left(\frac{1}{r^+} + \frac{1}{r^-}\right)\left(\frac{1}{\varepsilon_{ref}} - \frac{1}{\varepsilon_s}\right) \quad (2)$$

The oxidation potential of the porphyrin donor ($E^{ox}(D)$) determined by cyclic voltametry is 1.1 V (vs. SCE in MeCN) while the reduction potentials for the TCQ and BQ species ($E^{red}(A)$) are −0.07 V and −0.64 V (vs. SCE in MeCN), respectively [14]. The radii of the molecular ions used were r^+ = 4.8 Å [15] and r^- = 4.06 Å from calculation [3]. The excitation energy (E_{00}) was determined from the onset of the porphyrin absorption spectrum. However, a key parameter in determining the driving force for electron transfer is the appropriate donor–acceptor separation (R_c). Rather than the centre-to-centre chromophore distance it is often considered more correct to use the chromophore edge-to-edge separation that defines the closest interaction for the molecular orbitals of the interact-

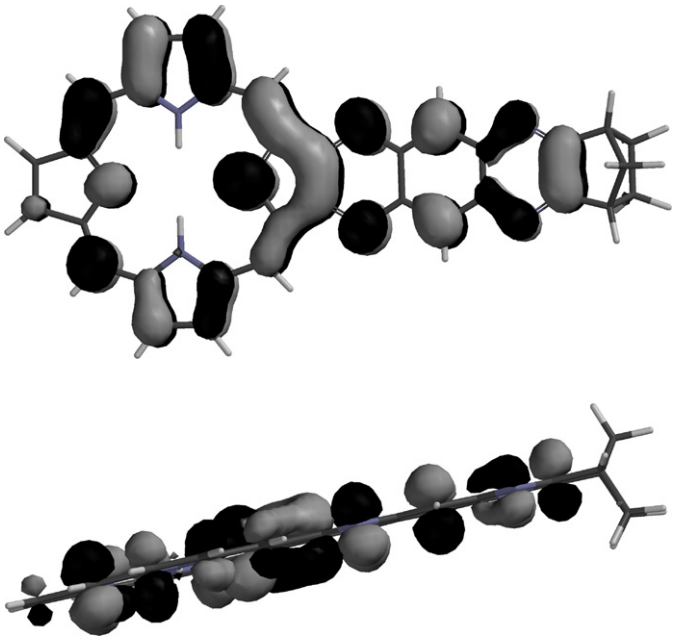

Fig. 2. Two views of the B3LYP/6-31G(d)//AM1 LUMO molecular orbital for the porphyrin-tetraazaanthracene component of the dyads illustrating extensive penetration of the LUMO into the tetraazaanthracene component of the bridge. Because of the N–H···H–N interactions across the porphyrin ring, the AM1 optimized geometry turned out to possess C_1 symmetry, which explains the slight deviation of the LUMO from the expected A' (C_s) symmetry.

ing species. The extent of distribution of the molecular orbitals of the porphyrin into the tetraazaanthracene three aromatic six membered rings that make up part of the linking bridge is particularly relevant in this regard. If the chromophore LUMO extends to encompass this aromatic section of the bridge then the donor–acceptor separation should correctly take this in to account. The molecular orbitals for the porphyrin-tetraazaanthracene were calculated at the B3LYP/6-31G(d) level with the geometry optimized at the AM1 level of theory. The results of the calculation (see Fig. 2) show that the LUMO does indeed extend into the conjugated bridge and has significant amplitude right to the extremity of the aromatic section. Interestingly it was found that neither the HOMO nor the HOMO-1 extends into the conjugated section of the bridge.

For comparison purposes the driving force calculations reported in Table 1 were performed using three different donor–acceptor separations—18.05 Å, 13.24 Å and 7.32 Å. These separations correspond, respectively to the distances determined from the optimized structures for centre-to-centre (porphyrin-to-acceptor), edge-to-edge (porphyrin-to-acceptor) and edge-to-edge (porphyrin-tetraazaanthracene-to-acceptor). It is apparent from Table 1 that for these molecules the donor–acceptor separation used has a strong influence on predicting whether charge separation will occur in particular solvents. In Table 1 the free energy for charge recombination (ΔG_{CR}) is also reported and has been calculated using the following equation:

$$\Delta G_{CR} = -(E_{00} + \Delta G_{CS}) \quad (3)$$

With increasing solvent polarity the driving force for charge separation increases while that for charge recombination shows the opposite trend as expected. Of particular note is the prediction that, at the donor–acceptor separation of 7.32 Å, corresponding to the distance from the edge of the teraaza-anthracene aromatic rings to the nearest edge of the acceptor, charge separation is possible in all solvents for **P[6]TCQ** but should only occur in those solvents in Table 1 more polar than toluene ($\varepsilon_s = 2.39$) when BQ is the acceptor.

Absorption spectra recorded in the porphyrin region of the dyads were identical to the model porphyrin compound without acceptor (**P[6]**) indicating that there are no strong ground state donor–acceptor interactions perturbing the electronic spectra. The absorption spectra for the **P[6]TCQ** dyad and the model porphyrin compound in hexane are provided in Fig. 3(a) as an example. Steady-state and time-resolved fluorescence measurements of the porphyrin dyads and the model porphyrin fluorophore showed strong quenching of the porphyrin fluorescence in **P[6]TCQ** in all solvents investigated (e.g. >90% quenched, see Fig. 3(b)) while for **P[6]BQ** significant quenching was observed only in acetonitrile and benzonitrile. The rates for PET (k_{PET}) can be calculated using Eq. (4) where τ_{fm} is the

Table 1
Free energy change for photoinduced charge separation (ΔG_{CS}) and charge recombination (ΔG_{CR}) for **P[6]TCQ** and **P[6]BQ** in solvents of different polarity (ε_s) [16] and at various donor–acceptor (D–A) separations calculated using the Weller equation (see text)

Solvent	ε_s	E_{00} (eV)	ΔG_{CS} (eV)			ΔG_{CR} (eV)		
			18.05 Å	13.24 Å	7.32 Å	18.05 Å	13.24 Å	7.32 Å
P[6]TCQ								
Acetonitrile	36.6	1.87	−0.72	−0.73	−0.75	−1.15	−1.14	−1.12
Benzonitrile	25.9	1.87	−0.69	−0.70	−0.74	−1.18	−1.17	−1.14
THF	7.52	1.88	−0.47	−0.51	−0.63	−1.41	−1.37	−1.26
Toluene	2.39	1.88	+0.24	+0.12	−0.25	−2.12	−2.00	−1.63
n-Hexane	1.89	1.88	+0.51	+0.36	−0.11	−2.39	−2.24	−1.77
P[6]BQ								
Acetonitrile	36.6	1.87	−0.15	−0.16	−0.18	−1.72	−1.71	−1.69
Benzonitrile	25.9	1.87	−0.12	−0.13	−0.17	−1.75	−1.74	−1.71
THF	7.52	1.88	+0.01	+0.06	−0.06	−1.98	−1.94	−1.83
Toluene	2.39	1.88	+0.81	+0.69	+0.32	−2.69	−2.57	−2.20
n-Hexane	1.89	1.88	+1.08	+0.93	+0.46	−2.96	−2.81	−2.34

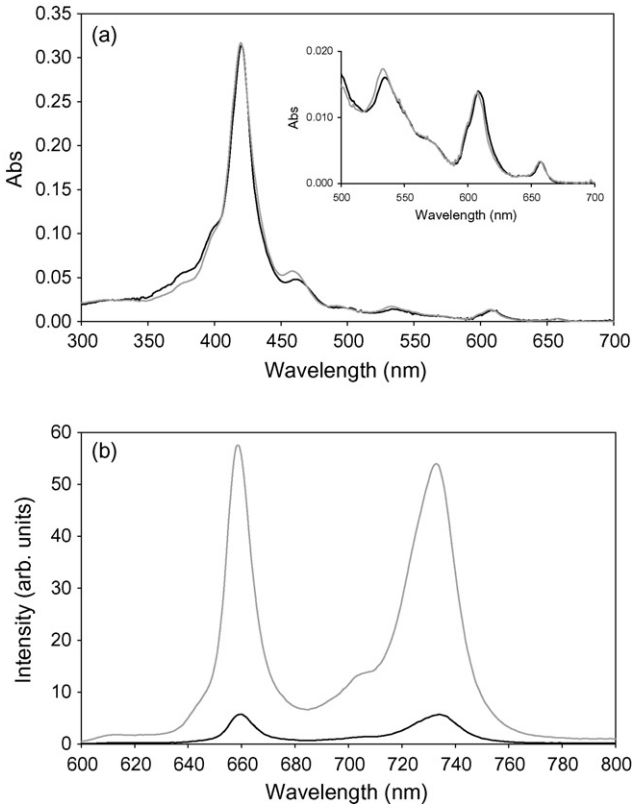

Fig. 3. (a) Absorption spectra of the model porphyrin **P[6]** (grey line) and **P[6]TCQ** (black line) in *n*-hexane. (b) Fluorescence spectra for the model porphyrin **P[6]** (grey line) and **P[6]TCQ** (black line) in *n*-hexane, excitation wavelength 607 nm.

lifetime of the model porphyrin compound without the acceptor and τ_f the lifetime of the relevant dyad,

$$k_{PET} = \left(\frac{1}{\tau_f}\right) - \left(\frac{1}{\tau_{fm}}\right) \quad (4)$$

The data are summarized in Table 2. The fluorescence decay profiles of the model compound in each solvent were single exponential but where quenched emission was observed from the dyads a double exponential fit was required with the major component (>93%) associated with a short decay time and a minor long-lived (ns) contribution attributed to residual emission from the presence of a small concentration of unlinked porphyrin chromophores. For the case of **P[6]TCQ** in the polar and non-polar solvents studied, the major component of the fluorescence decays had a lifetime of less than 50 ps associated with a very efficient quenching process with rates greater than $2 \times 10^{10}\ s^{-1}$. The lifetimes reported in Table 2 for **P[6]TCQ** obtained from reconvolution analysis of the fluorescence decay profiles are at the resolution limits of time-correlated single photon counting and have an estimated uncertainty of 20 ps so no particular significance can be attributed to the small differences in the very short lifetimes extracted. Energy transfer from the porphyrin donor to the acceptors is energetically not feasible for these molecules and thus the results are consistent with a PET process being responsible for the quenching process

Table 2
Fluorescence lifetime (τ_F) data and calculated rates for photoinduced electron transfer (k_{PET}) for **P[6]BQ** and **P[6]TCQ** in different solvents

	P[6]TCQ		**P[6]BQ**	
	τ_F (ns)[a]	k_{PET} (s^{-1})[b]	τ_F (ns)[a]	k_{PET} (s^{-1})[b]
PhCN	0.024	3.3×10^{10}	3.5	1.6×10^{8}
THF	0.030	4.2×10^{10}	–	–
Toluene	<0.020	$>5 \times 10^{10}$	–	–
n-Hexane	0.020	5.0×10^{10}	–	–

[a] There was a small (<7%) contribution of a longer-lived (nanosecond) component attributed to residual unlinked porphyrin chromophores.

[b] k_{PET} rates were calculated using Eq. (4) where the fluorescence lifetime of the model porphyrin chromophore **P[6]** was 7.8 ns, 11.2 ns, 10.3 ns and 12.1 ns in PhCN, THF, toluene, and hexane, respectively.

Nanosecond flash photolysis studies were also carried out in a range of solvents to investigate the charge-separated state recombination kinetics. With the time resolution of the instrument (approximately 8 ns) a transient associated with TCQ radical anion ($TCQ^{\bullet -}$) could only be observed in non-polar solvents following excitation of the porphyrin chromophore in **P[6]TCQ** at 534 nm. The transient absorption spectrum (Fig. 4) shows minima at 610 nm and 540 nm, associated with ground state depletion of the porphyrin, and a transient with maximum observed at 570 nm that was identified as $TCQ^{\bullet -}$ by comparison with the absorption spectrum of the chemically reduced (with $NaBH_4$) TCQ model compound. No radical ion

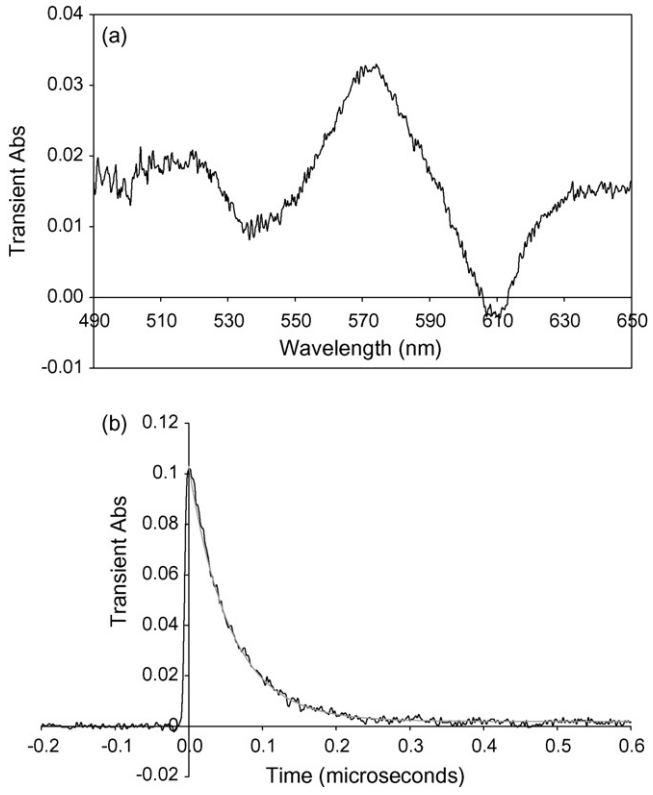

Fig. 4. (a) Transient absorption spectrum of **P[6]TCQ** in *iso*-pentane, 70 ns after excitation at 534 nm. The absorption band at 570 nm is associated with the TCQ radical anion. (b) Transient decay of **P[6]TCQ** in *iso*-pentane after excitation at 534 nm (black line), included is the fit to a single exponential decay with a 57 ns lifetime and a small (2%) offset (grey line).

transients could be detected for **P[6]BQ** although the presence of considerable porphyrin triplet state formation for the partially quenched compound could have masked some radical ion formation. The results suggest that charge recombination must be very fast ($>10^8\ s^{-1}$) for solvents more polar than toluene for **P[6]TCQ**. The lifetime of the $TCQ^{\bullet -}$ transient of **P[6]TCQ** exhibits a marked solvent dependence. The transient observed in *iso*-pentane (dielectric constant [16], $\varepsilon_s = 1.85$), *n*-hexane ($\varepsilon_s = 1.89$), methyl cyclohexane ($\varepsilon_s = 2.02$) and toluene ($\varepsilon_s = 2.39$) decayed with a single exponential lifetime of 56 ns, 49 ns, 27 ns and <8 ns, respectively, showing a remarkable sensitivity to solvent. Ultrafast transient absorption measurements on sub-nanosecond timescales that are able to probe the CR reaction in polar solvents will be the subject of a separate investigation.

4. Discussion

The results demonstrate the high efficiency of the PET process for the TCQ acceptor compared to BQ. The fluorescence quenching data are also generally consistent with the predictions of the Weller calculations reported in Table 1 (using the appropriate 7.32 Å donor–acceptor separation), that PET is thermodynamically feasible for **P[6]TCQ** in all solvents under investigation while only in the more polar solvents should charge separation occur with BQ as an acceptor. It is interesting to note that the PET process with TCQ as acceptor is extremely efficient over a wide range of solvent polarities. The Marcus [17,18] description for electron transfer reactions predicts a parabolic dependency of the kinetic barrier to ET, $\Delta G^{\#}_{CS}$, on the driving force and solvent reorganisation energy, λ, given by the following equation:

$$\Delta G^{\#}_{CS} = \frac{(\Delta G_{CS} + \lambda)^2}{4\lambda} \quad (5)$$

The reorganisation energy can be broken into two components, one arising from the molecule's response to ET, λ_i, and one from the solvent's response, λ_s. λ_i is largely independent of solvent polarity and is typically of the order of 0.1–0.4 eV for donor–acceptor molecules such as those investigated here and a value of 0.3 eV has been assumed for both the systems studied herein [19]. λ_s for the transfer of one electron has been estimated using a simple model assuming point charges in a dielectric continuum given by the following equation:

$$\lambda_s = \frac{1}{4\pi\varepsilon_0}\left[\frac{1}{2r_D} + \frac{1}{2r_A} - \frac{1}{R_c}\right]\left[\frac{1}{n^2} - \frac{1}{\varepsilon_s}\right] \quad (6)$$

The total reorganisation energy in PhCN is calculated to be 0.88 eV while in *n*-hexane it is 0.3 eV ($\lambda_s = 0$). Eq. (5) predicts a significant value of 0.15 eV for $\Delta G^{\#}_{CS}$ for PET from P to BQ for **P[6]BQ** in PhCN consistent with the observation that the PET process only partially quenches the fluorescence emission of the porphyrin for this system. For TCQ as acceptor in **P[6]TCQ**, however, $\Delta G^{\#}_{CS}$ is calculated to be much smaller at 0.006 eV placing the PET reaction in the "barrierless" region compared to BQ which occurs in the "normal" region. Furthermore, even though the driving force is reduced at low polarity, $\Delta G^{\#}_{CS}$ for **P[6]TCQ** remains very small due to the much lower

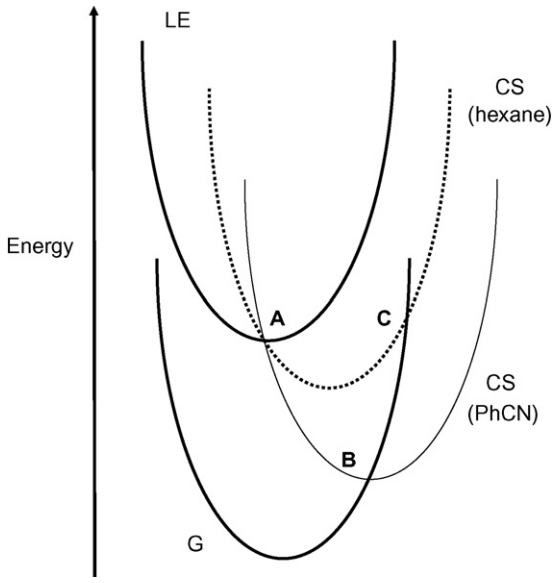

Fig. 5. Schematic of the suggested potential energy surfaces for **P[6]TCQ** showing the origin of the energy barrier for charge recombination in non-polar solvents. The ground (G) state, locally excited (LE) state and charge-separated (CS) state in a polar solvent (PhCN) and a non-polar solvent (hexane) are shown. Region A indicates that the forward CS reaction occurs in the "barrierless" region for both polar and non-polar solvents. For the polar solvent CR is also 'barrierless' (region B). Increasing the driving force for CR by using a non-polar solvent leads to a substantial barrier (region C) and much slower CR indicating that for non-polar solvents CR occurs in the "inverted" region.

reorganisation energy and the PET reaction is predicted to be "barrierless" for all solvent polarities from MeCN through to *iso*-pentane. This is in agreement with experimental observations that k_{PET} for **P[6]TCQ** is greater than $2 \times 10^{10}\ s^{-1}$ in all solvents investigated. This situation is schematically illustrated at "A" in Fig. 5 where the parabolic potential energy surfaces for the charge-separated (CS) state in both hexane and PhCN intersect the locally excited (LE) state near its minimum.

The Marcus equation (Eq. (5)) also helps to explain the strong solvent dependence of the charge-separated state lifetime of **P[6]TCQ**. The driving force ($-\Delta G_{CR}$) for charge recombination in polar solvents (acetonitrile and PhCN) is only about 1.1 eV and assuming that $|\lambda|$ is the same for the CS and CR processes, the barrier for CR, $\Delta G^{\#}_{CR}$, is estimated to be only 0.019 eV in PhCN and MeCN. This shows that the CR reaction lies close to the barrierless region for these solvents resulting in ultrafast charge recombination rates consistent with there being no CS transient species detected in the nanosecond flash photolysis experiments. As solvent polarity decreases, $-\Delta G_{CR}$ increases (Table 1) and in non-polar solvents is >1.5 eV. Under these conditions, $\Delta G^{\#}_{CR}$ is predicted to increase substantially indicating that charge recombination lies in the 'inverted' region in these solvents. The two situations of barrierless CR in polar solvents and inverted region CR in non-polar solvents are schematically represented in Fig. 5 at "B" and "C", respectively. The actual values returned by the Marcus equation for $\Delta G^{\#}_{CR}$ in *iso*-pentane, *n*-hexane and methylcyclohexane are of the order of 1.7–1.9 eV which are likely to be considerable overestimates due to the difficulties of using the solvation model of

point charges in a dielectric continuum for highly non-polar conditions. However, the prediction of there being a considerable kinetic barrier to CR in the non-polar alkane solvents is consistent with the relatively long CS lifetimes observed and the CS lifetimes demonstrate the predicted relationship for inverted region ET remarkably well: as ΔG_{CR} decreases with increasing solvent polarity, k_{CR} increases and the CS lifetime decreases.

There should be no direct overlap of the molecular orbitals of the donor and acceptor even at the closest edge-to-edge (porphyrin-tetraazaanthracene-to-acceptor) separation of 7.32 Å, suggesting that the electronic coupling, V, required for electron transfer to occur is mediated by the σ-orbitals of the linking polynorbornane bridge. Rigid bridges of this type have been shown previously to be extremely effective in promoting such 'through-bond' coupling in PET reactions, even over inter-chromophore separations exceeding 12 Å [1,2,7,8,11,19,20]. Indeed, the electronic coupling through a six-bond polynorbornane bridge has been measured to be as high as 112 cm^{-1} [21]. The coupling in the systems studied here can be extracted from the non-adiabatic rate equation (in its high temperature limit) for weakly coupled ET reactions [17,18],

$$k_{ET} = \frac{4\pi^2}{h\sqrt{4\pi\lambda_s k_B T}}|V|^2 \exp\left[\frac{-(\Delta G_{CS} + \lambda)^2}{4\lambda k_B T}\right] \quad (7)$$

Substitution of the experimentally determined values for **P[6]BQ** in PhCN (where they are most reliable both in terms of calculated driving force (polar conditions) and measured PET rate constant) yields a coupling of 14 cm^{-1}. This is typical of many polynorbornane linked systems. For a k_{PET} value of 5×10^{10} s^{-1} and using the ΔG_{CS} values at 7.32 Å separation (Table 1), the calculated coupling is also in the range of 15–20 cm^{-1} for all solvents for **P[6]TCQ**. As discussed above, due to the limitations of the solvation model used, a quantitative estimation of the coupling for charge recombination in the non-polar solvents cannot be made. However it might be expected that V_{CR} would be considerably less than V_{CS} since recombination is to the ground state and involves the HOMO orbital of the porphyrin moiety which the calculations show does not extend into the linking bridge in the manner of the LUMO orbital. Thus both the reduced coupling and the presence of a significant kinetic barrier may contribute to the observed CS lifetimes.

5. Conclusion

The **P[6]TCQ** molecular dyad studied in this work represents a molecular system where very efficient forward PET mediated by through-bond coupling occurs in both polar and non-polar solvents. Charge recombination exhibits a strong solvent dependence with the extended lifetimes observed in non-polar solvents characteristic of Marcus inverted region behaviour. The ratio of forward to back electron transfer rates ($k_{PET}/k_{CR} = 2500$) for **P[6]TCQ** in the non-polar solvent *iso*-pentane is substantial for a simple dyad suggesting it may be a useful structural component in molecular photovoltaic devices.

Acknowledgements

The corresponding authors (KPG and MNP-R) acknowledge financial support from the Australian Research Council (ARC) under the Discovery Grant Program, SJL acknowledges the award of an ARC Postdoctoral Fellowship and TDMB acknowledges the award of an Australian Postgraduate Award. TG is grateful to the University of Melbourne for the provision of a Visiting Scholars Award. MNP-R thanks the Australian Partnership for Advanced Computing and the Australian Centre for Advanced Computing and Communications for allocation of time.

References

[1] M.N. Paddon-Row, Adv. Phys. Org. Chem. 38 (2003) 1–85.
[2] J.W. Verhoeven, J. Photochem. Photobiol. C 7 (2006) 40–60.
[3] K.P. Ghiggino, J.A. Hutchison, S.J. Langford, M.J. Latter, M.A.P. Lee, P.R. Lowenstern, C. Scholes, M. Takezaki, B.E. Wilman, Adv. Funct. Mater. 17 (2007) 805–813.
[4] D.M. Guldi, Chem. Soc. Rev. 31 (2002) 22–36.
[5] J. Wiberg, L. Guo, K. Pettersson, D. Nilsson, T. Ljungdahl, J. Mårtensson, B. Albinsson, J. Am. Chem. Soc. 129 (2007) 155–163.
[6] V. Balzani, A. Credi, M. Venturi, Molecular Devices and Machines—A Journey into the Nano World., Weinheim: Wiley–VCH, Cambridge, 2003.
[7] M.N. Paddon-Row, Aust. J. Chem. 56 (2003) 729–748.
[8] K.P. Ghiggino, A.H.A. Clayton, J.M. Lawson, M.N. Paddon-Row, New J. Chem. 20 (1996) 853–859.
[9] T.D.M. Bell, K.P. Ghiggino, K.A. Jolliffe, M.G. Ranasinghe, S.J. Langford, M.J. Shephard, M.N. Paddon-Row, J. Phys. Chem. A 106 (2002) 10079–10088.
[10] T.D.M. Bell, K.A. Jolliffe, K.P. Ghiggino, A.M. Oliver, M.J. Shephard, S.J. Langford, M.N. Paddon-Row, J. Am. Chem. Soc. 122 (2000) 10661–10666.
[11] T.D.M. Bell, T.A. Smith, K.P. Ghiggino, M.G. Ranasinghe, M.J. Shephard, M.N. Paddon-Row, Chem. Phys. Lett. 268 (1997) 223–228.
[12] P.T. Gulyas, S.J. Langford, N.R. Lokan, M.G. Ranasinghe, M.N. Paddon-Row, J. Org. Chem. 62 (1997) 3038–3039.
[13] A. Weller, Z. Phys. Chem., Neue Folge 133 (1982) 93–98.
[14] D.F. Rothenfluh, A.M. Oliver, M.N. Paddon-Row, J. Chem. Soc. Perkin Trans. 2 (1996) 639–648.
[15] r^- was determined from the molecular volume of tetracyanonaphthoquinidodimethane calculated at the HF/6-31G(d)//HF/3-21G level.
[16] J.A. Dean, Solvent dielectric constants quoted were measured at 20 °C with the exception of THF measured at 22 °C, in: Lange's Handbook of Chemistry, 15th ed., McGraw-Hill, New York, 1999.
[17] R.A. Marcus, Angew. Chem. Int. Ed. Engl. 32 (1993) 1111–1121.
[18] R.A. Marcus, N. Sutin, Biochim. Biophys. Acta 811 (1985) 265–322.
[19] M.N. Paddon-Row, Acc. Chem. Res. 27 (1994) 18–25.
[20] H. Oevering, M.N. Paddon-Row, H. Heppener, A.M. Oliver, E. Cotsaris, J.W. Verhoeven, N.S. Hush, J. Am. Chem. Soc. 109 (1987) 3258–3269.
[21] H. Oevering, J.W. Verhoeven, M.N. Paddon-Row, J.M. Warman, Tetrahedron 45 (1989) 4751–4766.